Journal of Organometallic Chemistry, 475 (1994) 233–240

Cooperative effects in π-ligand bridged dinuclear complexes

XV. * Heterodinuclear Fe-Co complexes from mononuclear η^5-cyclooctatrienyl iron complexes

Ulrich Behrens, Jürgen Heck and Michiel Maters

Institut für Anorganische und Angewandte Chemie, Universität Hamburg, Martin-Luther-King-Platz 6, D-22146 Hamburg (Germany)

Gerlinde Frenzen

Fachbereich Biologie / Chemie, Universität Gesamthochschule Kassel, Heinrich-Pett-Str. 40, D-34109 Kassel (Germany)

Annie Roelofsen and Harry T. Sommerdijk

Vakgroep Anorganische en Algemene Chemie, Universiteit Nijmegen, Toernooiveld, NL-6525 ED Nijmegen (Netherlands)

(Received January 17, 1994)

Abstract

The reaction of CpFe(1–5-η-C_8H_8-8-*exo*-R) (R = $CH(CO_2Et)_2$: **2a**; R = H: **2b**) with $CpCo(C_2H_4)_2$ at $T \leq 40$°C yields the diamagnetic heterodinuclear, *cyclo*-C_8 bridged FeCo complexes [{(CpFe)(CpCo)}μ-(η^7-C_8H_8R)] (R = $CH(CO_2Et)_2$: **3**; R = H: **4a**) which are thermally labile. For **3** the substituent R = $CH(CO_2Et)_2$ is thermally cleaved with increasing temperature yielding the paramagnetic ESR active 35 valence electron (ve) compound [{(CpFe)(CpCo)}μ-Cot] (**5**). The ESR data of **5** indicate a cobalt localized unpaired electron. **5** is easily oxidized by O_2, $[Ph_3C]BF_4$ or $[FeCp_2]PF_6$ yielding the stable diamagnetic 34 ve cation [{(CpFe)(CpCo)}μ-Cot]$^+$ ($\mathbf{5}^+$). Crystal structure analysis of $\mathbf{5}BF_4$ establishes a synfacial $\eta^5:\eta^5$ coordination with a very long Fe–Co distance of about 287(1) pm which is assumed to be too long for a Fe–Co single bond. The cyclic voltammetry study of $\mathbf{5}^+$ reveals two chemically as well as electrochemically reversible redox couples $\mathbf{5}/\mathbf{5}^+$, $\mathbf{5}^+/\mathbf{5}^{2+}$ and one quasi-reversible redox couple $\mathbf{5}^-/\mathbf{5}$. Evidence for the formation of the radical dication $\mathbf{5}^{2+}$ containing a Co-centred unpaired electron, can be got from *in situ* ESR measurements. The thermal lability of **4a** leads irreversibly to the isomeric complex **4b** at elevated temperature. The activation energy ΔE_a of this molecular transformation was estimated by ^{1}H NMR spectroscopy as 103 kJ/mol. Preliminary crystal structure determinations of the high temperature isomer **4b** confirm a synfacial 1,2,6,7-η:3–5-η bonding mode for the cyclooctatrienyl ligand. The cyclooctatrienyl ligand of the low temperature isomer **4a** is assumed to coordinate via a 1-η:6,7-η-bonding mode to the Co centre whereas the coordination mode of the *cyclo*-C_8 ligand to the Fe centre should occur in 2-5-η fashion. C_s molecular symmetry for **4a**, which can be deduced from the ^{1}H NMR spectra, is explained by a low energy twitching motion of **4a**.

Key words: Iron; Cobalt; Cyclooctatetraene; Electrochemistry; Electron spin resonance; x-ray diffraction

1. Introduction

The heterodinuclear electron-poor μ-cyclooctatetraene (Cot) complexes [(CpCr)(L_nM)μ-Cot] (L_n = Cp, $(CO)_3$; M = V, Cr, Mo, W, Fe, Co) have been prepared with CpCr(η^6-Cot) as starting material [2,3]. CpCr(η^6-Cot) contains one free double bond which can function as an entrance for a second metal ligand fragment. However, attempts to prepare electron-richer μ-Cot complexes with [CpFe(η^6-Cot)]PF_6 (**1**) as the precursor compound failed, although this also contains a free double bond in the Cot ligand [4]. This disadvantage may be due to the cationic nature of **1**. Hence, to circumvent problems possibly caused by the charge, the nucleophile adducts of **1**, CpFe(1-5-η-C_8H_8-8-exo-R)-

Correspondence to: Prof. Dr. J. Heck.

* For Part XIV see ref. [1].

0022-328X/94/$7.00
SSDI 0022-328X(94)24530-V

($R = CH(CO_2Et)_2$: **2a**; R = H: **2b**) were used as the starting material, as these are neutral and possess an uncoordinated double bond [5]. As a CpM transfer reagent, $CpCo(C_2H_4)_2$ [6] was chosen.

2. Results and discussion

The reactions of **2a** and **2b** with $CpCo(C_2H_4)_2$ yield the heterodinuclear complexes [(CpFe)(CpCo)μ-C_8H_8-R] ($R = CH(CO_2Et)_2$: **3**; R = H: **4a**) in acceptable yields (Scheme 1, a). **3** and **4a** are thermally labile. In the case of **3** the thermal lability becomes apparent from the cleavage of the substituent $R = CH(CO_2Et)_2$ with increasing temperature, and the 35 ve complex [{(CpFe)(CpCo)}μ-Cot] (**5**) is obtained (Scheme 1, b). **5** is paramagnetic, ESR active (*vide infra*) and extremely sensitive to oxygen. Therefore, **5** can easily be oxidized by air, $[Ph_3C]BF_4$ or $[FeCp_2]PF_6$ forming the stable diamagnetic cation $\mathbf{5}^+$. The reduction of $\mathbf{5}^+$ with sodium amalgam yields **5** again (Scheme 1, c).

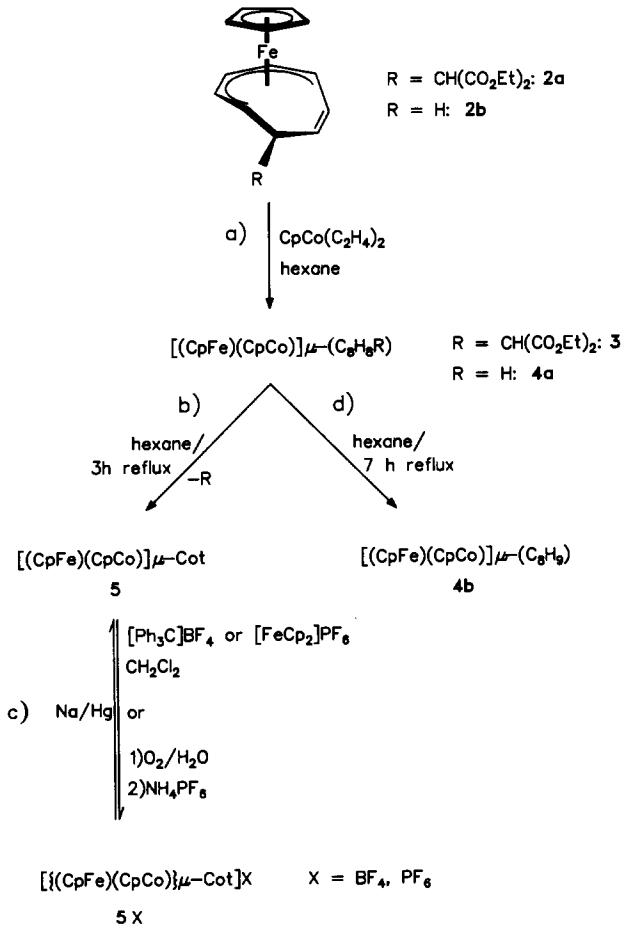

Scheme 1.

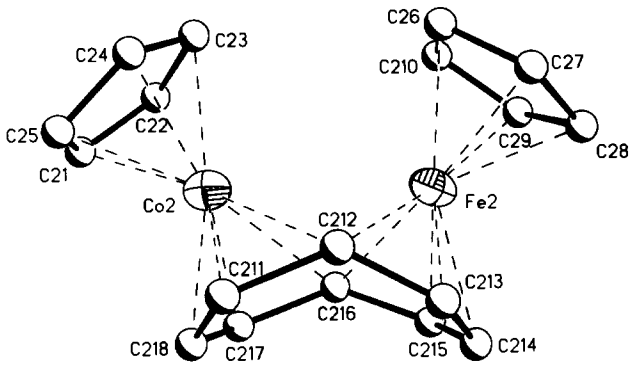

Fig. 1. Molecular structure of $5BF_4$. Only one of the three molecules per asymmetric unit is shown (the hydrogen atoms are omitted for clarity, the metal atoms are shown as 50% thermal ellipsoids; concerning the assignment of Fe and Co see Experimental part). Selected bond lengths (pm) (the bond lengths of the two other molecules are in parentheses): Co1–Fe1 286.3(4) [288.1(5), 286.5(4)]); Co1–C111 198(2) [204(2), 198(2)]; Co1–C118 198(2) [197(2), 207(2)]; Co1–C117 198(2) [202(2), 202(2)]; Co1–C116 241(2) [241(2), 250(2)]; Co1–C112 258(2) [255(2), 238(2)]; Fe1–C112 223(2) [222(2), 233(2)], Fe1–C113 204(2) [200(2) 199(2); Fe1–C114 201(3) [204(2), 208(2)]; Fe1–C115 198(3) [201(2), 202(2)]; Fe1–C116 233(2) [223(2), 225(2)]. The angle between the best planes defined by C111, C112, C116, C117 and C112, C113, C115, C116 amounts to 138°.

The crystal structure analysis of $5BF_4$ (Fig. 1, Tables 1 and 2) reveals a synfacial configuration with a pseudo mirror plane which contains the metal centres and bisects the Cot as well as the Cp ligands. The asymmetric unit has three different molecules $5BF_4$ with different Fe–Co distances ranging between 286.3(4) and 288.1(5) pm. These iron–cobalt distances are too long for a Fe–Co single bond; they are more than 10 pm longer than the longest known Fe–Co single bonds (*vide infra*) [7a], which are normally in the range 250–270 pm [7b,c]. The Cot ligand is coordinated in a $\eta^5:\eta^5$-bonding mode. The two η^5 planes of the Cot ligand enclose an angle of 138°. Based on this structure determination two resonance structures can be as-

TABLE 1. Principal experimental parameters of the crystal structure analysis and crystal data for [{(CpFe)(CpCo)}μ-Cot]BF_4 ($5BF_4$)

chem formula	$C_{18}H_{18}BCoF_4Fe$	space group	$P2_1/c$
fw	435.9	density g cm^{-3}	1.761
a, pm	2115.4(12)	abs. coeff. mm^{-1}	1.929
b, pm	1285.6(6)	indep. reflections	10834
c, pm	1832.7(8)	obs. reflections	2895 ($F > 3.0\sigma(F)$)
β, °	98.15(4)	*R*	0.0870
cell vol. pm$^3 \times 10^{-6}$	4934(4)	*wR*	0.0722
Z	12		

TABLE 2. Atomic coordinates ($\times 10^4$) and equivalent isotropic displacement coefficients ($Å^2 \times 10^3$)

	x	y	z	U_{eq} [a]
Co(1)	75(1)	2731(2)	1255(2)	32(1)
Fe(1)	682(1)	2723(3)	2754(2)	28(1)
Co(2)	−6642(2)	3108(2)	−4217(2)	34(1)
Fe(2)	−5948(2)	2191(2)	−5299(2)	31(1)
Co(3)	−3148(1)	3217(2)	−3416(2)	31(1)
Fe(3)	−2752(1)	3004(2)	−1862(2)	27(1)
C(11)	551(12)	4042(20)	879(13)	60(8)
C(12)	−89(12)	4010(18)	611(12)	49(7)
C(13)	−268(11)	3114(17)	171(12)	41(6)
C(14)	301(10)	2516(15)	212(11)	31(6)
C(15)	781(11)	3061(17)	625(11)	41(6)
C(16)	1417(10)	2925(18)	3618(12)	43(6)
C(17)	1666(11)	2676(19)	2942(12)	50(7)
C(18)	1482(11)	3491(19)	2448(14)	56(8)
C(19)	1080(12)	4212(20)	2733(14)	60(8)
C(110)	1076(11)	3841(19)	3469(13)	55(8)
C(111)	−664(9)	2782(16)	1808(10)	27(5)
C(118)	−649(10)	1826(16)	1418(11)	34(6)
C(117)	−90(10)	1251(16)	1465(11)	31(6)
C(116)	463(11)	1265(16)	2008(12)	37(6)
C(115)	540(12)	1205(19)	2796(14)	58(8)
C(114)	172(12)	1695(20)	3254(14)	59(8)
C(113)	−160(10)	2596(16)	3170(11)	34(6)
C(112)	−343(10)	3162(18)	2473(12)	45(7)
C(21)	−6749(12)	3476(21)	−3163(13)	62(8)
C(22)	−6261(12)	2804(20)	−3113(13)	59(8)
C(23)	−6502(11)	1886(19)	−3481(12)	47(7)
C(24)	−7168(12)	2075(19)	−3700(12)	53(7)
C(25)	−7298(12)	3053(19)	−3520(12)	53(7)
C(26)	−6034(11)	719(17)	−4897(13)	44(7)
C(27)	−6021(12)	669(18)	−5637(14)	51(7)
C(28)	−5433(10)	1094(16)	−5786(12)	37(6)
C(29)	−5108(12)	1378(17)	−5097(13)	47(7)
C(210)	−5464(11)	1174(17)	−4548(14)	50(7)
C(211)	−7218(12)	3518(18)	−5160(12)	56(8)
C(212)	−6961(10)	2671(18)	−5575(12)	44(7)
C(213)	−6568(11)	2777(19)	−6124(13)	52(7)
C(214)	−5980(10)	3289(16)	−6105(12)	36(6)
C(215)	−5577(11)	3596(16)	−5470(12)	40(7)
C(216)	−5760(10)	3754(16)	−4781(12)	35(6)
C(217)	−6237(10)	4410(16)	−4548(11)	27(6)
C(218)	−6887(9)	4366(16)	−4800(10)	26(6)
C(31)	−3843(9)	2037(17)	−3550(11)	33(6)
C(32)	−3546(10)	2153(17)	−4184(11)	35(6)
C(33)	−3650(9)	3174(16)	−4457(11)	29(6)
C(34)	−4018(10)	3728(17)	−3964(11)	39(6)
C(35)	−4127(10)	3002(18)	−3425(12)	50(7)
C(36)	−3481(13)	1995(21)	−1701(14)	73(9)
C(37)	−3604(12)	3004(20)	−1490(13)	63(8)
C(38)	−3144(10)	3222(19)	−943(12)	43(7)
C(39)	−2723(11)	2445(16)	−830(12)	38(7)
C(310)	−2900(11)	1671(19)	−1320(12)	52(7)
C(311)	−2241(9)	2913(16)	−3492(11)	29(6)
C(312)	−2216(10)	2387(17)	−2801(11)	41(7)
C(313)	−1893(10)	2642(17)	−2112(12)	41(6)
C(314)	−1820(12)	3553(19)	−1713(13)	58(8)
C(315)	−2272(12)	4368(19)	−1839(13)	57(8)
C(316)	−2767(13)	4540(18)	−2454(13)	59(8)
C(317)	−2688(11)	4593(19)	−3238(13)	52(7)
C(318)	−2342(10)	3955(17)	−3676(12)	35(6)
B(2)	4924(3)	9637(5)	2421(4)	41(8)
F(5)	4366	9948	2639	62(6)
F(6)	4913	9855	1693	61(6)
F(7)	5420	10148	2821	100(8)
F(8)	4998	8595	2530	71(6)
B(1)	1947(6)	−57(10)	4502(7)	82(18)
F(1)	2154	489	5125	115(17)
F(2)	2440	−202	4111	119(17)
F(3)	1473	481	4085	107(16)
F(1A)	1959	−23	3763	234(34)
F(2A)	2548	81	4863	135(20)
F(3A)	1561	711	4695	147(22)
F(4)	1720	−996	4686	127(10)
B(3)	1284(5)	9712(9)	559(6)	76(12)
F(9)	1597	9070	141	132(10)
F(10)	648	9685	311	85(16)
F(11)	1504	10700	509	67(15)
F(12)	1391	9395	1273	129(20)
F(10A)	1091	10580	165	161(18)
F(11A)	1683	9986	1177	63(11)
F(12A)	767	9212	752	111(14)

[a] Equivalent isotropic U defined as one third of the trace of the orthogonalized U_{ij} tensor.

cribed without a Fe–Co bond warranting 18 ve for each metal centre:

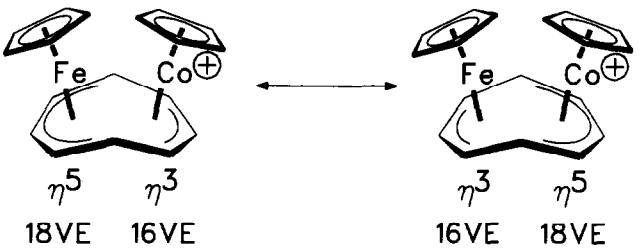

These resonance structures are in accordance with the Cot-carbon–metal distances: the bond lengths between the metal centres and the bridging carbon atoms C*z*12 and C*z*16 ($z = 1$–3) are distinctly longer than those between the metal centres and the internal Cot-carbon atoms C*z*11, C*z*13–C*z*15, C*z*17 and C*z*18 ($z = 1$–3) (Fig. 1). In contrast to this coordination mode, the ^{1}H-, ^{13}C-NMR spectra only show one Cot resonance signal indicating a fast rotation of the Cot ligand on the NMR time scale.

To get a deeper insight into the metal–metal interaction in **5**, cyclic voltammetry studies were performed. **5**BF_4 exhibits a well-defined oxidation and reduction step at 0.0 V and at −1.45 V (*vs.* Ag/Ag^+), respectively (Fig. 2, Table 3). Both steps are chemically as well as electrochemically reversible one-electron transfer processes. A second, quasi-reversible reduction step is at −2.66 V. Unfortunately, limitations imposed by the solvent prevent the exact determination of the ratio

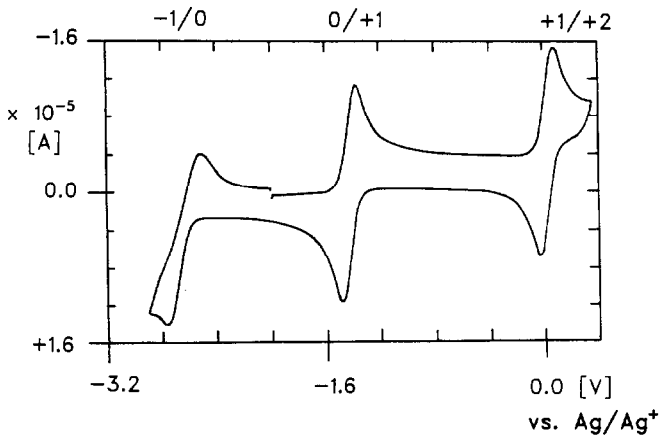

Fig. 2. Cyclic voltammogram of [{(CpFe)(CpCo)}μ-Cot]BF_4 ($5BF_4$) (DME, 0.1 M [$^nBu_4$]PF_6, Pt working electrode, *vs.* Ag/Ag^+, 0.1 M Ag triflate).

i_b/i_f. Hence, the redox chemistry of **5** follows the redox cascade:

$$5^- \rightleftarrows 5 \rightleftarrows 5^+ \rightleftarrows 5^{2+}$$

Interestingly, the oxidation and the first reduction potential are almost identical to those of the corresponding mononuclear sandwich compound cobaltocene [8] indicating two almost independent metal centres in the corresponding dinuclear species. The potential of the redox couple $5^+/5^{2+}$ is rather more shifted to positive potentials than it is for ferrocene, which could be a result of the inductive effect of the first positive charge. The more electron-deficient nature of the 33 ve dication 5^{2+} will cause a stronger direct metal–metal interaction [2].

Whereas the neutral and monocationic species are sufficiently stable to be isolated and fully characterized, the only spectroscopic evidence for 5^{2+} comes from *in situ* ESR measurement at low temperature ($T \leq 230$ K) (Fig. 3). In liquid solution, the ESR spectrum (Fig. 3, **A**) only shows an asymmetrical envelope signal without ^{59}Co hyperfine structure (hfs) which may be due to comparable ^{59}Co hf coupling constants (hfcc)

TABLE 3. Cyclic voltammetry data of [{(CpFe)(CpCo)}μ-Cot]BF_4 ($5BF_4$) [a]

redox couple	$E_{1/2}$ [b] [V]	ΔE [mV]	i_b/i_f [c]
+1/+2	+0.003(3)	85	1.0
0/+1	−1.45(3)	85	1.0
−1/0	−2.66	170	[d]

[a] $E_{equilibrium}$ ($5BF_4$) = −950 mV, T = 20°C.
[b] v = 100 mV/s, *vs.* Ag/Ag^+ (0.1 M [($^nBu)_4N$]PF_6 in DME, working electrode: Pt, reference electrode: Ag/0.1 M Ag triflate in DME).
[c] i_b: peak current of the backward scan, i_f: peak current of the forward scan.
[d] Difficult to determine because of limitations of the solvent.

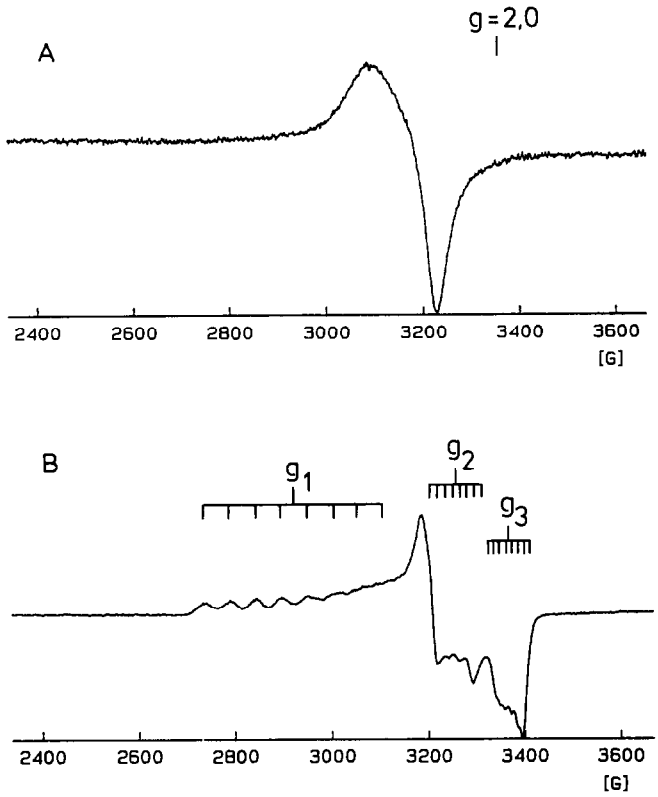

Fig. 3. X-band ESR-spectra of [{(CpFe)(CpCo)}μ-Cot]$^{2+}$(5^{2+}), recorded *in situ* during the electrochemical generation of 5^{2+}; **A**: liquid solution spectrum (toluene, T = 230 K); **B**: solid solution spectrum (T = 15 K) (acetone, 0.1 M [$^nBu]_4PF_6$).

and line widths. The large peak-to-peak line width $\Delta B_{p/p}$ = 143 G is in accord with the distinct g and ^{59}Co hf anisotropy of 5^{2+} that becomes clear from the rigid solution spectrum (Fig. 3, **B**, Table 4). The g and ^{59}Co hf anisotropy and the magnitude of the ^{59}Co hfcc of 5^{2+} point to a non-degenerate ground state with a Co-centred unpaired electron [9].

The paramagnetic neutral complex **5** also contains one unpaired electron, and the spectra and ESR data

TABLE 4. ESR data of [{(CpFe)(CpCo)}μ-Cot] (**5**), 5^{2+} and [CpCoCot]$^-$ (**7**) [10]

	5^{2+}	**5**	**7**
g_1	2.30	2.19	2.20
$A_1(^{59}Co)$ [G]	52	43	46
g_2	2.06 [a]	2.04	2.02
$A_2(^{59}Co)$ [G]	23 [a]	48	41
g_3	1.99 [a]	1.99	1.95
$A_3(^{59}Co)$ [G]	12 [a]	46	41
⟨g⟩	2.12	2.07	2.06

[a] g_2, g_3 and the corresponding ^{59}Co hfcc were only determined approximately due to the low resolution of the spectrum in this region.

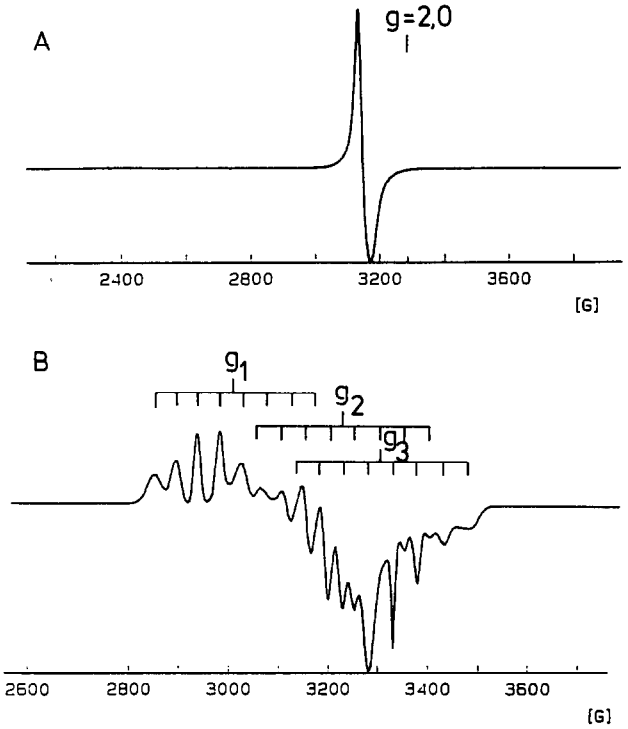

Fig. 4. X-band ESR-spectra of [{(CpFe)(CpCo)}μ-Cot] (**5**); **A**: liquid solution spectrum (toluene, $T = 220$ K); **B**: solid solution spectrum (toluene, $T = 40$ K).

are comparable to 5^{2+}. The liquid solution ESR-spectrum shows one broad asymmetrical signal ($\Delta B_{p/p} = 30$ G) void of any ^{59}Co hfs (Fig. 4, **A**). As for 5^{2+}, the ^{59}Co hf coupling constant is apparently of the order of magnitude of the line width. In comparison with 5^{2+}, the reduced line width of the liquid solution spectrum of **5** agrees with the less pronounced g anisotropy that emerges from the frozen solution spectrum of **5**. Nevertheless, the g anisotropy and the ^{59}Co hfcc still indicate a metal centred unpaired electron (Table 4, Fig. 4, **B**).

The ESR data for **5** reveal a remarkable agreement with those of the mononuclear radical anion [CpCoη^4-Cot]$^-$ (**7**) [10] (Table 4), showing that the frontier orbitals of both types of complexes are very similar. Hence, in contradiction to the original interpretation [10], **7** can be described as a 17 ve complex with the negative charge localized in the uncoordinated penta-

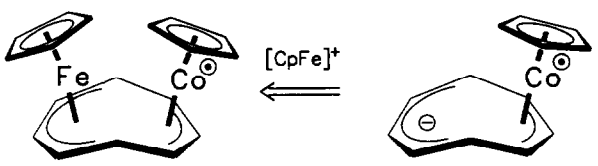

Scheme 2.

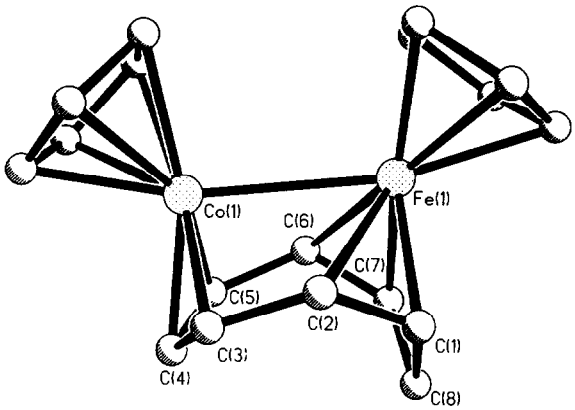

Fig. 5. Molecular structure of **4b**. Fe–Co bond length: 273.4(1) pm (for more information see ref. 11).

dienyl part of the Cot ring (Scheme 2). In the case of the dinuclear FeCo complex **5** this pentadienyl anion is stabilized by the coordination of the $CpFe^+$ unit. To confirm the structure of **5**, which is the first dinuclear, synfacial 35 ve Cot complex (Scheme 2), Mössbauer studies are in progress.

The second heterodinuclear complex **4a** (Scheme 1) does not lose the substituent R as shown for **3**, but undergoes an irreversible haptotropic rearrangement to isomer **4b** at elevated temperature (Scheme 1, d).

From ^{1}H NMR spectra (Experimental section) it becomes obvious that both isomers **4a** and **4b** should have a molecular C_s symmetry, at least a time-averaged C_s symmetry with respect to the NMR time scale. Unfortunately, no suitable crystals of the low temperature isomer **4a** have been obtained for structure analysis. However, a preliminary crystal structure determination of the high temperature isomer **4b** [11 *] indicates a pseudo mirror plane containing the metal centres as well as C4 and C8 of the C_8H_9-ring. The cyclooctatrienyl ligand is coordinated to the metal centres via a μ-(1,2,6,7-η : 3–5-η) bonding mode (Fig. 5).

Hence, the molecule consists of a CpCp(η^3-allyl) unit and a CpFe(η^4-diene) fragment wherein the two double bonds are isolated by a CH_2 group. On account of the Fe–Co distance of 273.4(1) pm and the diamagnetism of **4b**, a Fe–Co single bond has to be considered warranting 18 ve for each metal centre. Nevertheless, it has to be mentioned that the Fe–Co bond length in **4b** is one of the longest known Fe–Co single bonds [7]. The structure of the kinetically controlled isomer **4a** still remains unclear but as a suggestion a 2–5-η : 1,6,7-η bonding mode is outlined in Scheme 3, which results in a molecular C_1 symmetry. For this

* Reference number with asterisk indicates a note in the list of references

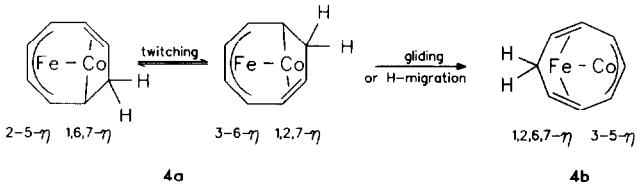

Scheme 3.

kind of hapticity in synfacial dinuclear Cot and cyclooctatriene complexes a twitching process has recently been shown [12,13], simulating a molecular time-averaged C_s symmetry which is in accordance with the ^1H NMR spectra.

With increasing temperature the twitching process could change to a gliding process (Scheme 3, a), and as a result, the high temperature product **4b** is formed. Alternatively, a metal-assisted hydrogen migration may occur to form **4b** (Scheme 3, b). For the activation energy E_a of the rearrangement is estimated at 103 kJ/mol which is comparable with the activation barrier of the hydrogen shift in (tricarbonyl)(η^6-cycloheptatriene)chromium (1031 kJ/mol) [14], the hydrogen migration seems the more likely process.

3. Experimental details

All manipulations were carried out under nitrogen with thoroughly dried solvents. The electrochemical and ESR studies were performed as described recently [2a]. The *in situ* ESR study in a SEERS cell has been published elsewhere [15]. $CpCo(C_2H_4)_2$ and CpM(1-5-η-C_8H_8-8-*exo*-R) (R = $CH(CO_2Et)_2$: **2a**; R = H: **2b**) were prepared according to literature methods [6,5].

3.1. Preparation of [{(CpFe)(CpCo)}μ-$C_8H_8CH(CO_2Et)_2$] (3)

0.92 (5.1 mmol) of $CpCo(C_2H_4)_2$ was added to a stirred solution of 1.6 g (4.2 mmol) of **2a** in 130 ml of hexane. After stirring at 40°C for 7 h, 205 ml ethene was formed. The reaction solution was cooled to +6°C and the precipitate was isolated, dried and dissolved in a minimum amount of toluene. Addition of hexane and storage at −30°C for two days revealed 0.26 g (12%) of **3**. Found: C, 58.5; H, 5.3. $C_{25}H_{28}CoFeO_4$ (508.25) calcd.: C, 59.09; H, 5.55%. Because of the thermal lability which leads to the paramagnetic compound **5**, the ^1H NMR spectrum of **3** shows a considerable line broadening which does not allow a complete assignment. Nevertheless, the Cp signals of the CpCo and CpFe units as well as most of the signals of the *cyclo*-C_8 protons and the signals of the Et substituents could be assigned: δ 4.75, 3.96 (Cp); 4.43 (2H), 3.43 (1H), 2.97 (1H), 2.55 (2H), 2.46 (2H) (*cyclo*-C_8); 4.0 (CH_2–CH_3), 0.95 (CH_2–CH_3).

3.2. Preparation of [(CpFe)(CpCo)]μ-Cot (5)

0.72 g (4 mmol) of $CpCo(C_2H_4)_2$ was added to a stirred solution of 1.84 g (4.8 mmol) of **2a** in 100 ml of hexane, and the reaction mixture was stirred for 16 h at 40°C. In the meantime 140 ml ethene was formed. After refluxing for an additional 3 h, the dark solution was stored overnight at −30°C. Filtration yielded 0.89 g of dark brown material of crude **5**. **5** was purified by oxidation and subsequent reduction with sodium amalgam (*vide infra*).

3.3. Preparation of {[(CpFe)(CpCo)]μ-Cot}$^+BF_4$ (5BF_4)

0.91 g (2.8 mmol) of $[Ph_3C]BF_4$ were added to a stirred solution (−80°C) of 0.89 g (2.6 mmol) of **5** in dichloromethane. After stirring for one hour, the dark purple solution was allowed to warm to room temperature. The crude product was precipitated by addition of Et_2O. The solid material was collected on a filter frit and extracted with acetonitrile. The extract was evaporated to dryness, and the residue was re-dissolved in dichloromethane. The product was precipitated by addition of Et_2O. Yield: 0.85 g (70% based on **2a**) of **5**BF_4. Found: C, 48.6; H, 4.5. $C_{18}H_{18}BCoF_4Fe$ (435.90) Calcd: C, 49.59; H, 4.16%. IR (nujol): ν 1046 cm^{-1} (s, BF_4). ^1H NMR ([D_3]acetonitrile): δ 5.54s, Cp(Co), 5H), 4.81 (s, Cot, 8H), 4.79 (s, Cp(Fe), 5H). ^{13}C NMR ([D_3]acetonitrile): δ = 87.9 (CpCo), 83.5 (CpFe), 60.6 (Cot). FAB-MS: *m/z*(%) 349(100) [M^+], 387(5), 284(6) [M^+ − Cp], 245(7) [M^+ − Cot], 228(7) [M^+ − CpFe], 189(27) [M^+ − FeCot], 154(28), 136(25), 107(9).

3.4. Preparation of {[(CpFe)(CpCo)]μ-Cot}PF_6 (5PF_6)

980 mg (2.9 mmol) of $[FeCp_2]PF_6$ was added to a dichloromethane solution of 1.01 g (2.9 mmol) of **5**. The solution immediately turned purple. After stirring for an additional 30 min, the purple solution was filtered and restricted. After addition of Et_2O and cooling to −30°C 1.22 g (85%) of **5**PF_6 as purple crystals could be obtained.

5PF_6 was also obtained by the oxidation of a toluene solution of **5** in air. The cation 5^+ could be extracted with water. Addition of an excess of NH_4PF_6 to the water solution yielded **5**PF_6 as a dark violet microcrystalline material (further purification: see above). Found: C, 43.8, H, 3.7. $C_{18}H_{18}CoF_6FeP$ (494.06) Calcd: C, 43.76; H, 3.67%. IR (nujol): ν 827 (s, PF_6), 557 (s, PF_6). ^1H NMR ([D_3]acetonitrile): δ 5.54 (s, Cp(Co), 5H), 4.81 (s, Cot, 8H), 4.79 (s, Cp(Fe), 5H).

3.5. Preparation of [{(CpFe)(CpCo)}μ-Cot] (5) by reduction of 5PF$_6$

450 mg (0.9 mmol) of **5**PF$_6$ were added to a stirred suspension of 2.02 g sodium amalgam (1%) in 60 ml of THF. After stirring the solution for 4 h the dark brown solution was cooled to −40°C and decanted from solid Hg. The solvent was stripped off *in vacuo*, and the residue was dissolved in toluene. Restriction of the solution and cooling to −30°C gave 290 mg (87%) of dark brown crystalline powder of **5**. Found: C, 61.4; H, 5.7. $C_{18}H_{18}CoFe$(349.77) Calcd.: C, 61.89; H, 5.20. **5** has been additionally characterized as BF_4 salt by oxidation with $[Ph_3C]BF_4$ (see 3.3).

3.6. Preparation of [{(CpFe)(CpCo)}μ-C_8H_9] (4a)

420 mg (2.3 mmol) of $CpCo(C_2H_4)_2$ were added to a stirred solution of 380 mg (1.7 mmol) of $CpFe(\eta^5\text{-}C_8H_9)$ (**2b**) in 100 ml hexane. After stirring for 16 h, the dark green solution was filtered, restricted and cooled to −30°C. After filtration 299 mg (50%) of **4a** as a dark green material has been isolated. Found: C, 61.23; H, 5.32. $C_{18}H_{19}FeCo$ (350.12) Calcd.: C, 61.75; H, 5.47%. ^{1}H NMR ([D_6]benzene): δ 4.69 (s, Cp, 5H), 4.48 (t, 2H), 4.20 (s, Cp, 5H), 3.95 (t, 1H), 3.38 (t, 2H), 1.92 (m, 2H), 1.27 (t, 1H), −1.12 (dt, 1H). EI-MS: *m/z*(%) 350(16) [M^+], 284(12) [M^+ − CpH], 244(18) [$M^+ - C_8H_9$], 229(38) [M^+ − CpFe], 226(46), 189(84) [$M^+ - FeC_8H_9$], 186(62), 160(20), 137(23), 124(91) [$M^+ - CpFeC_8H_9$], 121(85) [$M^+ - CpCoC_8H_9$], 115(11), 104(16) [$M^+ - Cp_2FeCoH$], 103(20), 98(19), 91(22), 78(26), 76(32), 65(31), 59(67) [$M^+ - Cp_2CoC_8H_9$], 56(100) [$M^+ - Cp_2FeC_8H_9$].

3.7. Preparation of [{(CpFe)(CpCo)}μ-C_8H_9] (4b)

250 mg (1.4 mmol) of $CpCo(C_2H_4)_2$ was added to a stirred solution of 280 mg (1.2 mmol) of $CpFe(\eta^5\text{-}C_8H_9)$ (**2**) in 50 ml hexane. After stirring for 16 h, the dark green solution was refluxed for 7 h. The solution was evaporated to dryness, the residue was extracted with a minimum amount of toluene, and the toluene solution was cooled to −30°C for three days. After filtration 340 mg (69%) of **4b** as a dark green crystalline material has been obtained. Found: C, 61.68; H, 5.30. $C_{18}H_{19}FeCo$ (350.12) Calcd.: C, 61.75; H, 5.47%. ^{1}H-NMR ([D_6]benzene): δ 4.81 (s, Cp, 5H), 4.21 (t, 2H), 3.92 (s, Cp, 5H), 2.73 (t, 1H), 2.54 (t, 2H), 2.41 (dt, 1H), 2.28 (q, 2H), 0.18 (dt, 1H). EI-MS: *m/z*(%) 350(28) [M^+], 284(22) [M^+ − CpH], 244(38) [$M^+ - C_8H_9$], 229(73) [M^+ − CpFe], 225(37), 189(79) [$M^+ - FeC_8H_9$], 186(63), 160(13), 137(33), 124(100) [$M^+ - CpFeC_8H_9$], 121(86) [$M^+ - CpCoC_8H_9$], 115(28), 104(26) [$M^+ - Cp_2FeCoH$], 103(23), 98(16), 91(30), 78(24), 77(26), 65(41), 59(68) [$M^+ - Cp_2CoC_8H_9$], 56(69) [$M^+ - Cp_2FeC_8H_9$].

3.8. Determination of the activation energy E_a of the thermal rearrangement of 4a

Four NMR tubes were each filled with a 0.3 M [D_8] toluene solution of **4a**, and were sealed under vacuum. Each NMR sample was tempered at a different temperature (50, 60, 70 and 78°C, respectively). The progress of the thermolysis was followed by recording of ^{1}H NMR spectra in course of time. The ratio of **4a** and **4b** was determined measuring the integrals of the Cp resonance signals. From these data a first order reaction was found, and the activation energy E_a was calculated by means of a least squares best fit of an Arrhenius plot: E_a = 103 kJ/mol.

3.9. Crystal structure determination of 5BF$_4$

3.9.1. Crystal preparation

Suitable crystals of **5**BF$_4$ were grown by slow recrystallization from dichloromethane. A dark violet brown crystal was chosen with the approximate dimension 0.07 × 0.07 × 0.22 mm^3. On account of the inertness against air the crystal was mounted directly.

3.9.2. Data collection and refinement

Intensity data were collected in ω-scan mode on a Siemens R3m/V diffractometer at T = 193 K with graphite monochromated Mo Kα radiation.

The structure was solved by direct methods and subsequent difference Fourier synthesis. The full-matrix least squares refinement with isotropic displacement factors for all atoms except the metal atoms yielded a *R*-factor of 0.087 for 2895 reflections with $I < 3\sigma$ [16]. The hydrogen atoms were refined using a riding model with fixed temperature factors. The principal experimental parameters of the crystal structure analysis and crystal data are collected in Table 1.

The assignment of the metal centres Fe and Co was made because an exchange of these positions leads to worse *R*-values and considerably larger temperature factors. A better refinement of the structure was hampered by the weakly diffracting crystal and by the disorder of the BF_4 ions.

Further details of the structure determination can be obtained upon request from the Fachinformationszentrum Karlsruhe, Gesellschaft für wissenschaftlich-technische Information mbH, D-76344 Eggenstein-Leopoldshafen, giving reference to the depository number CSD-400601 and citing the authors and this paper.

Acknowledgement

This work was supported by the European Commission, Science Project CT 910 740. We would like to

thank Mrs. Y. Piprek for practical assistance and BASF for donation of Cot.

References and notes

1 J. Heck, K.-A. Kriebisch, W. Massa and S. Wocadlo, *J. Organomet. Chem.*, submitted.

2 (a) P.M.J.A. Hermans, A.B. Scholten, E.K. van den Beuken, H.C. Brussaard, A. Roelofsen, B. Metz, E.D. Reijerse, P.T. Beurskens, W.P. Bosman, J.M.M. Smits and J. Heck, *Chem. Ber., 126* (1993) 553;
(b) J. Heck, P.M.J.A. Hermans, A.B. Scholten, W.P.J.H. Bosman, G. Meyer, T. Staffel, R. Stürmer and M. Wünsch, *Z. Anorg. Chem., 611* (1992) 35.

3 B. Bachmann, F. Hahn, J. Heck and M. Wünsch, *Organometallics, 8* (1989) 2523.

4 J. Heck and W. Massa, *J. Organomet. Chem., 376* (1989) C15.

5 J. Heck, P.T. Beurskens, W.P. Bosman, H.C. Brussaard, R.J.M. Klein Gebbink, M. Maters and J.M.M. Smits, *J. Organomet. Chem., 469* (1994) 197.

6 K. Jonas and C. Krüger, *Angew. Chem., 92* (1980) 513; *Angew. Chem. Int. Ed. Engl., 19* (1980) 520.

7 (a) D.J. Chandler, R.A. Jones, A.L. Stuart and T.C. Wright, *Organometallics, 3* (1984) 1380; F. Richter and H. Vahrenkamp, *Organometallics, 1* (1982) 756.
(b) D.A. Roberts and G.L. Geoffroy in G. Wilkinson, F.G.A. Stone and E.W. Abel (eds.), *Comprehensive Organometallic Chemistry*, Pergamon Press, New York, Vol. 6, 1982, p. 763 ff;
(c) M.P. Jensen, D.A. Phillips, M. Sabat and D.F. Shriver, *Organometallics, 11* (1992) 1859.

8 S.P. Gubin, S.A. Smirnova and L.I. Denisovich, *J. Organomet. Chem., 30* (1971) 257 (in CH_3CN *vs.* SCE); A.J. Bard, E. Garcia, S. Kukharenko and V.V. Strelets, *Inorg. Chem., 32* (1993) 3528.

9 J.H. Ammeter, Ch. Elschenbroich, T.J. Groshens, K.J. Klabunde, O. Kühne and R. Möckel, *Inorg. Chem., 24* (1985) 3307.

10 T.A. Albright, W.E. Geiger, Jr., J. Moraczewski and B. Tulyathan, *J. Amer. Chem. Soc., 103* (1981) 4787.

11 The crystal structure analysis of **4b** was performed at 173 K with Mo K_α radiation. The crystal structure was refined with all independent 4063 reflections, but the refinement was hampered by a disorder of the molecules. The disorder was caused by two different sets of molecules of **4b** which vary in the direction of the Co–Fe vector by 180°. Although the structure could be refined to $R_1 = 0.045$, taking this disorder into account, the metal–carbon and the carbon–carbon bond lengths are not reliable. Nevertheless, the metal–metal distance could be estimated quite exactly, and the found hapticity of the C_8H_9 ligand is definitive and in agreement with the ^1H NMR spectrum.

12 J.H. Bieri, T. Egolf, W. von Philipsborn, U. Piantini, R. Prewo, U. Ruppli and A. Salzer. *Organometallics 5,* (1986) 2413.

13 F.A. Cotton, D.L. Hunter and P. Lahuerta, *J. Am. Chem. Soc., 97* (1975) 1046.

14 W.R. Roth and W. Grimme, *Tetrahedron Lett.*, (1966) 2347.

15 J.G.M. van der Linden, J. Heck, B. Walther and H.-C. Böttcher, *Inorg. Chim. Acta, 217* (1994) 29.

16 G.M. Sheldrick, SHELXTL PLUS, *Release 4.2 for Siemens R3 Crystallographic Research Systems*, Siemens Analytical X-Ray Instruments, Inc., Madison WI, USA, 1990.